

# A Systematic Approach to the Linear-Stability Assessment of Alfvén Eigenmodes in the Presence of Fusion-Born Alpha Particles for ITER-like Equilibria

P. Rodrigues<sup>1</sup>, A. Figueiredo<sup>1</sup>, J. Ferreira<sup>1</sup>, R. Coelho<sup>1</sup>, F. Nabais<sup>1</sup>, D. Borba<sup>1</sup>, N. F. Loureiro<sup>1</sup>, H. J. C. Oliver<sup>2</sup> and S. E. Sharapov<sup>3</sup>

<sup>1</sup>Instituto de Plasmas e Fusão Nuclear, Instituto Superior Técnico, Universidade de Lisboa, 1049-001 Lisboa, Portugal.

<sup>2</sup>HH Wills Physics Laboratory, Univ. of Bristol.

<sup>3</sup>EURATOM/CCFE Fusion Association, Culham Science Centre, Abingdon OX14 3DB, UK.

*Corresponding Author:* par@ipfn.ist.utl.pt

## Abstract:

A systematic approach to assess the linear stability of Alfvén eigenmodes in the presence of fusion-born alpha particles is described. Because experimental results for ITER are not available yet, it is not known beforehand which Alfvén eigenmodes will interact more intensively with the alpha-particle population. Therefore, the number of modes that need to be considered in stability assessments becomes quite large and care must be exercised when choosing the numerical tools to work with, which must be fast and efficient. In the presented approach, all possible eigenmodes are first found after intensively scanning a suitable frequency range. Each solution found is then tested to find if its discretization over the radial grid in use is adequate. Finally, the interaction between the identified eigenmodes and the alpha-particle population is evaluated with the drift-kinetic code CASTOR-K, in order to assess their growth rates and hence their linear stability. The described approach enables one to single out the most unstable eigenmodes in a given scenario, which can then be handled with more specialized tools. This selection capability eases the task of evaluating alpha-particle interactions with Alfvén eigenmodes, either for ITER scenarios or for any other kind of scenario planning.

## 1 Introduction.

Plasma heating in the ITER burning regime will be provided mainly by an isotropic population of fusion-born alpha particles, with thermal energy significantly higher than that of the bulk plasma species [1]. These supra thermal particles must be kept confined in the core, in order to keep the plasma burning and prevent the vessel's walls from sustaining serious damages. However, they can drive Alfvén eigenmodes (AEs) unstable,

which may then enhance their transport away from the core and direct them against the walls [2, 3, 4]. Therefore, to predict alpha-particle losses and wall loads, one has to develop efficient techniques to assess the linear stability of all relevant modes for a given plasma equilibrium configuration.

When modeling experimental results, measured data usually provide helpful guidance about which AEs are interacting with the fast-particle population. Present day diagnostics might provide the mode frequency, its radial location, and even its structure [3], narrowing considerably the number of modes that need to be taken into account. However, no such guidance is available when dealing with scenarios for which no experiments have been performed yet. Therefore, the number of modes that need to be taken into account, and have their interaction with the fast-particle population suitably evaluated, becomes quite large. In the following, a systematic approach is described to assess the linear stability of all AEs that can be present in a prescribed ITER-like equilibrium, within reasonable bounds for their frequencies and for their toroidal and poloidal mode numbers. Because the number of modes to be handled is potentially quite large, care must be exercised when choosing the numerical tools to work with, which must be fast and computationally efficient.

## 2 The proposed workflow.

Given a magnetic equilibrium configuration, its corresponding AEs are first found with the ideal-MHD code MISHKA [5], which is used to intensively scan a predefined range of normalized mode frequencies ( $0.01 \leq \omega/\omega_A \leq 2$ , where  $\omega_A = V_A/R_0$ ,  $R_0$  is the tokamak's major axis, and  $V_A$  is the on-axis Alfvén velocity). For each toroidal mode number in the range  $1 \leq n \leq 100$ , the frequency-scan procedure is as follows: First, the normalized-frequency interval is sampled with a constant step size  $\Delta(\omega/\omega_A) = 2 \times 10^{-5}$ ; Then, each frequency sample is used to provide MISHKA with a starting guess for the mode's eigenvalue, while keeping a solution *ansatz* with 17 poloidal harmonics ( $n - 1 \leq m \leq n + 16$ ); If the ensuing eigenvalue problem does not converge in a few iterations (in this case 7), the resulting solution is discarded and the next frequency sample is tried; Otherwise, the converged eigenmode is tested to find if its discretization over the radial grid in use ( $\Delta s = 1/501$ , with  $s^2 = \psi/\psi_b$ ,  $\psi$  the poloidal-field flux, and  $\psi_b$  its value at the boundary) is adequate; This procedure automatically excludes spurious, numerical-noise dominated solutions, as well as solutions with radial wavelengths shorter than that of the mesh size, and which cannot be adequately represented in the grid; In addition, solutions are also discarded if their frequency is found to match the Alfvén continuum somewhere within the plasma, since in such circumstances they are expected to undergo strong damping.

The frequency-scan phase ends up with a (possibly large) collection of AEs whose interaction with the fusion-born alpha population needs to be evaluated. This task is carried out with the drift-kinetic code CASTOR-K [6], which computes the energy transfer between a MHD perturbation of a given magnetic equilibrium and a population of particles described by some equilibrium distribution function. For every AE in the collection,

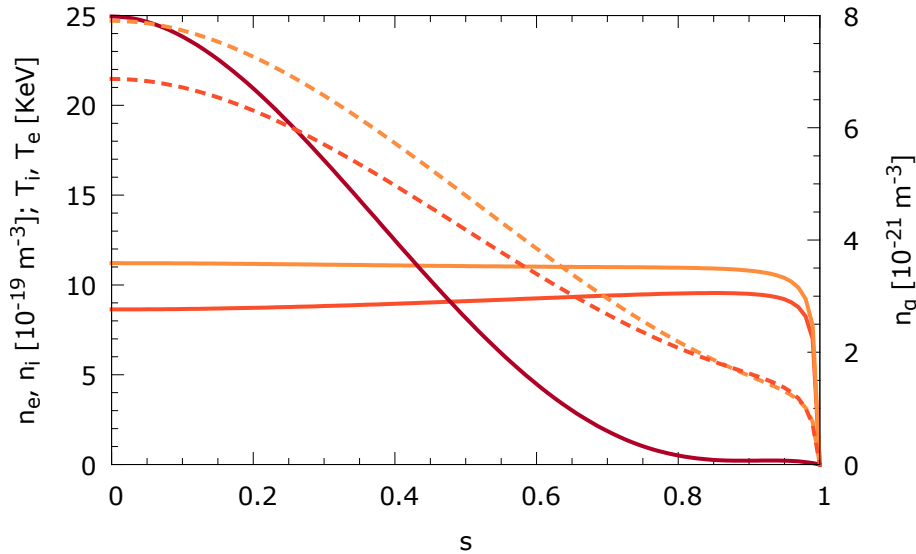


FIG. 1: Radial distributions of alpha-particles (solid red line), DT ion (dark orange) and electron (light orange) densities (solid lines), and temperatures (dashed lines).

CASTOR-K is run four times: first, to compute the drive due to fusion-born alpha particles described by a slowing-down energy distribution, and then once for each of the three thermal species (DT-ion mixture, electrons, and Helium ash). No radiative damping was considered in this analysis and the overall growth rate is taken to be the sum of all four contributions.

The sizable computational effort involved in the proposed scheme is essentially due to the very large number of AEs that need to be found by MISHKA and then processed by CASTOR-K, and not to individual instances of either code. Therefore, it falls into the category of trivially (or “embarrassingly”) parallel algorithms and a full parallelization of the proposed workflow was implemented in the HELIOS supercomputer [7], taking advantage of the independence of each AE processing. A typical workflow session in HELIOS, which involves finding and processing a few thousand AEs, takes about 12 to 15 hours if sufficient resources are available to allocate one AE to each computing node.

### 3 Results.

The results presented and discussed below were obtained for the ITER baseline scenario [8], with total plasma current  $I_p = 15$  MA, low shear safety-factor in the core region and  $q(0) = 0.987$ , peaked temperature profiles with  $T_i(0) = 21.5$  KeV for the DT ions and  $T_e(0) = 24.7$  KeV for the electrons, and flat density profiles (almost up to the edge) with  $n_e(0) = 11 \times 10^{-19} \text{ m}^{-3}$  and  $n_i(0) = 8.6 \times 10^{-19} \text{ m}^{-3}$  (FIG. 1). Fusion-born alpha-particles are well confined in the core region ( $s \lesssim 0.5$ ), with  $n_\alpha(0) = 7.9 \times 10^{-21} \text{ m}^{-3}$  and the highest gradient of their pressure contribution taking place at  $s \approx 0.42$ .

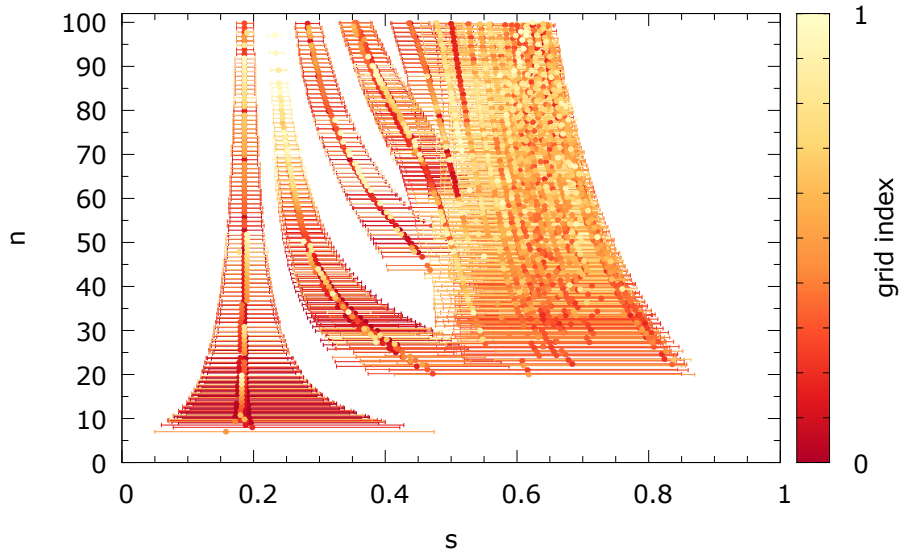


FIG. 2: AEs radial localization and width for each toroidal number  $n$ , colored by their respective grid index.

The frequency-scan procedure returns approximately 2300 distinct AEs, which are depicted in FIG. 2. There, the dots mark the radial location of each mode's highest peak and the lines mark its radial width. The color denotes the grid index, which indicates the increasing difficulty of a uniform radial grid with 501 points to describe modes with increasingly short-scale features. AEs with grid index greater than 1 were excluded from this plot and from further processing.

The results plotted in FIG. 2 agree, to a great extent, with analytical estimates of mode localization and width [9]. Notable exceptions are the near-vertical structure at  $s \approx 0.2$  and the structures ending at  $s \approx 0.275$  and  $s \approx 0.45$  for  $n \approx 100$ , which correspond to solutions outside the Toroidal Alfvén Eigenmode (TAE) frequency gap. Another difference is the absence of modes in the left and right upper corners, which is caused by having the AE's *ansatz* limited to 17 poloidal harmonics. Other structures present in reference [9] are not displayed in FIG. 2 because the grid index of their AEs exceeds the maximum value allowed. On the other hand, the absence of AEs for low toroidal mode numbers [ $n \lesssim 20$  for TAEs and  $n \lesssim 10$  for Ellipticity Alfvén Eigenmodes (EAEs)] is due to the particular density profile: being flat almost up to the edge, the density profile in FIG. 1 causes  $V_A$  (and hence the Alfvén-continuum frequency  $\omega = k_{\parallel} V_A$ ) to drop considerably in that region ( $s \gtrsim 0.8$ ). This effectively closes the outer end of the frequency gap and removes possible modes, located or extending into there, by continuum damping.

In the next step, the linear stability of all AEs in the collection is assessed with the CASTOR-K code. For almost all AEs, the energy exchange is dominated by alpha particles or DT ions (energetic particles from NBI or ICRH were not considered), whereas electrons or Helium ash have only negligible contributions. Three frequency gaps are clearly visible in FIG. 3, each with two branches (top and bottom): TAEs for  $\omega/\omega_A \approx 0.5$ ,

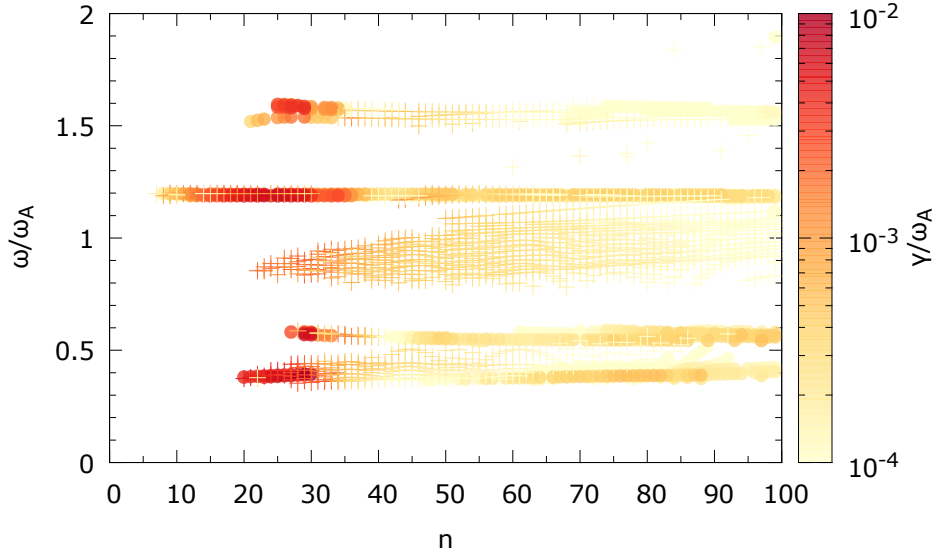


FIG. 3: AEs frequency distribution by toroidal number  $n$ , colored by their respective growth (dots) or damping (crosses) rates.

EAEs for  $\omega/\omega_A \approx 1$ , and Noncircular Alfvén Eigenmodes (NAEs) for  $\omega/\omega_A \approx 1.5$ . In all these three gaps, the largest growth rates are limited to the range  $20 \lesssim n \lesssim 30$ . Again, there are no TAEs (stable or not) up to  $n \approx 20$ . However, unstable EAEs in the top branch start at  $n \approx 10$ , while all bottom-branch EAEs are stable to alpha drive.

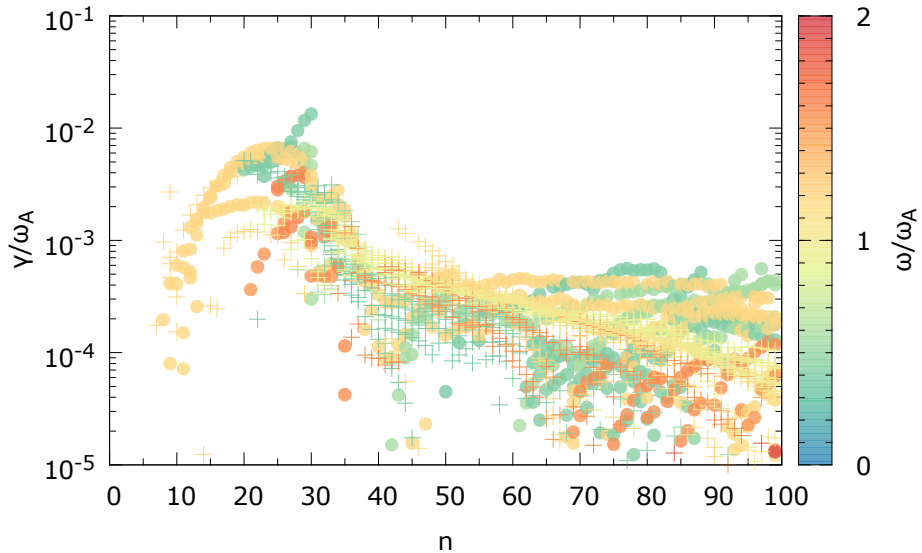


FIG. 4: AEs growth (dots) and damping (crosses) rate distribution by toroidal number  $n$ , colored by their respective normalized frequency.

The plot in FIG. 4 clearly shows that TAEs (greenish symbols) are the most unstable modes, with normalized growth rates in the range  $0.5\% \lesssim \gamma/\omega_A \lesssim 2\%$  (corresponding to  $1\% \lesssim \gamma/\omega \lesssim 3.5\%$ ). Moreover, and in accordance with previous estimates [9], the largest growth-rate value is attained at  $n = 30$ . On the other hand, top-branch EAEs (light orange) and NAEs (dark orange) have their growth rate limited to more modest ranges, these being, respectively,  $0.2\% \lesssim \gamma/\omega_A \lesssim 0.7\%$  and  $0.1\% \lesssim \gamma/\omega_A \lesssim 0.4\%$ . This being said, one should recall that radiative damping was not taken into account, which means that computed growth rates (particularly for large  $n$ ) may be overestimated.

The representation of the AEs' localization and extension can bring more insight if it is supplemented with additional information. In FIG. 5, unstable AEs are colored according to their normalized frequency, enabling one to easily identify which frequency ranges correspond to which radial structures. In particular, the near vertical structure at  $s \approx 0.2$  is seen to be made up of core-localized modes belonging to the top branch in the EAEs' gap. Interestingly, it shows also that the same radial structure can be shared by different frequency gaps, as is the case of core-localized TAEs and NAEs. If unstable AEs are colored by their growth rate instead, as in FIG. 6, it becomes readily obvious that the most unstable modes are short-width TAEs with  $20 \lesssim n \lesssim 30$  and localized around  $0.35 \lesssim s \lesssim 0.45$ . Incidentally, one should recall from FIG. 1 that the highest value of the alpha-pressure gradient takes place, precisely, at  $s \approx 0.42$ . The most unstable top-branch EAEs are also short-width modes in the same toroidal mode number range, but localized deeper into the core, at  $s \approx 0.2$ . Conversely, broad-width TAEs located at the outer half of the plasma ( $s \gtrsim 0.5$ ) are either close to marginal stability, stable, or interact with the Alfvén continuum, being thus excluded from the plot.

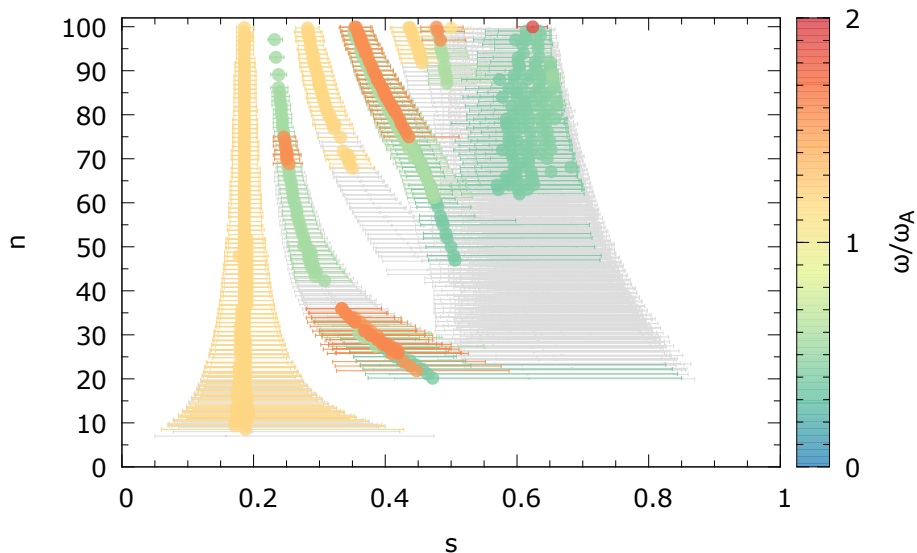


FIG. 5: Unstable AEs radial localization and width for each toroidal number  $n$ , colored by their respective normalized frequency. Grey lines indicate stable AEs.

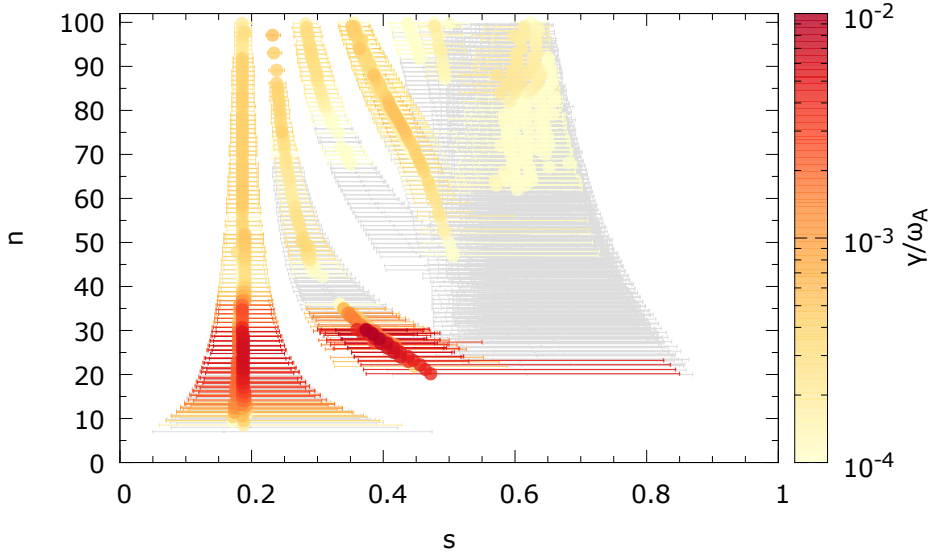


FIG. 6: Unstable AEs radial localization and width for each toroidal number  $n$ , colored by their respective growth rate. Grey lines indicate stable AEs.

## 4 Conclusions.

A systematic approach to assess the linear stability of AEs was presented that is particularly useful when dealing with scenarios for which no experimental guidance is available about which particular AEs interact more intensely with the fast particle population. In summary, it starts with an intensive scan of a frequency and toroidal mode-number ranges to identify all possible AE candidates, it is followed by a filtering stage to exclude non-physical solutions, and it ends with all selected AEs having their linear stability assessed by evaluating their energy exchange with the particle populations present in the plasma: fusion-born alphas, DT-ion mixture, electrons, and Helium ash. A judicious choice of the codes employed, which are fast and effective to accomplish their intended goals, allowed the designed workflow to be efficiently parallelized in order to take advantage of massively parallel computer systems. Its implementation in the supercomputer HELIOS clearly indicates that the techniques described above enable one to readily single out the most unstable AEs for a given scenario, which can then be studied with more specialized tools. This selection capability eases the task of evaluating alpha-particle interactions with Alfvén eigenmodes, either for ITER scenarios or for any other kind of scenario planning.

Regarding the specific ITER scenario used to test the proposed approach, it was found that most AEs with low toroidal mode number ( $n \lesssim 10$ ) interact with the Alfvén continuum and that most unstable modes occur for  $20 \lesssim n \lesssim 30$ , as predicted in earlier estimates [9]. While broad-width TAEs located outside the core ( $s \gtrsim 0.5$ ) were found to be either stable, close to marginal stability, or to interact with the Alfvén continuum, short-width TAEs located around the maximum of the alpha-pressure gradient ( $s \approx 0.42$ ) were found to be the most unstable ones in all the AE collection considered.

## Acknowledgments

All computations were carried out using the HELIOS supercomputer system at Computational Simulation Centre of International Fusion Energy Research Centre (IFERC-CSC), Aomori, Japan, under the Broader Approach collaboration between Euratom and Japan, implemented by Fusion for Energy and JAEA. This work was supported by the European Union's Horizon 2020 research and innovation programme under the grant agreement number 633053. IST activities were also supported by "Fundação para a Ciência e Tecnologia" through project Pest-OE/SADG/LA0010/2013. The views and opinions expressed herein do not necessarily reflect those of the European Commission.

## References

- [1] FASOLI, A., et al., Nucl. Fusion **47** (2007) S264.
- [2] BREIZMAN, B. and SHARAPOV, S. E., Plasma Phys. Control. Fusion **53** (2011) 054001.
- [3] SHARAPOV, S. E., et al., Nucl. Fusion **53** (2013) 104022.
- [4] NABAIS, F., et al., Nucl. Fusion **52** (2012) 083021.
- [5] MIHAILOVSKII, A., et al., Plasma Phys. Rep. **23** (1997) 844.
- [6] BORBA, D. and KERNER, W., J. Comp. Phys. **153** (1999) 101.
- [7] <http://www.iferc.org/csc/csc.html>
- [8] POLEVOI, A., et al., J. Fusion Res. SERIES **5** (2002) 82.
- [9] SHARAPOV, S. E. and OLIVER, H., "On Alfvén wave excitation in ITER baseline scenario with  $I_p = 15$  MA.", in preparation (2014).